Investigation of cross-phase modulation effect on upgraded NG-PON2 systems

YAN XU, SHUAI WANG*
Zaozhuang University, School of Opto-Electronic Engineering, Zaozhuang, China

Considering the rapid demands for bandwidth and the rare spectrum resources, there is an urgent need for upgrading the current NG-PON2 systems. In this paper, three upgradation methods are proposed including the bit rate increment from 10 Gb/s to 25 Gb/s per channel, the channel spacing decrement from 100 GHz to 50 GHz, and the increment in number of channels from 8 to 16. Moreover, the cross-phase modulation (XPM) effect on the upgradation methods is investigated. In the first case of increasing the bit rate to 25 Gb/s per channel, owing to the more-severe XPM effect induced by the bit rate increment, the XPM-induced sensitivity penalty is 2.3 dB. In the second case of decreasing the channel spacing to 50 GHz, the XPM effect causes a 0.4-dB sensitivity penalty. In the last case of increasing the number of channels to 16, an ignorable sensitivity penalty is induced to the system. The given results shall provide a reference in the formulation of future NG-PON2 standards.

(Received February 24, 2022; accepted August 10, 2022)

Keywords: Upgraded NG-PON2, Cross-phase modulation (XPM), Sensitivity penalty

1. Introduction

In recent years, with the emergence of new businesses and devices, such as ultra-high definition television, smart handheld devices, big data storage and cloud computing, the demands for bandwidth have been increased dramatically [1-4]. Currently, 10 Gb/s time division multiplexing passive optical network (TDM-PON) are widely operated. While, it is hard for the 10G TDM-PON to meet the growing needs of bandwidth. Therefore, in 2015, next-generation passive optical network stage 2 (NG-PON2) was proposed by the FSAN as the successor standard of gigabit-capable PON (GPON) or 10 gigabit-capable PON (XG-PON), and published as a standard of G.989.1 by ITU-T [5, 6]. The G.989.1 standard defines that the NG-PON2 can employ the structure of time and wavelength division multiplexed passive optical network (TWDM-PON) to improve the system capacity, where 4 or 8 wavelengths with 10-Gb/s bit rate per channel and 100-GHz channel spacing are used [7, 8]. Considering the rapid demands for bandwidth and the limited spectrum resources, operators are quite favorable in upgrading the current NG-PON2 [9]. In this paper, three potential upgradation methods for the next generation NG-PON2 are considered, including the bit rate increment to 25 Gb/s per channel (10 Gb/s for the current protocol), the channel spacing decrement to 50 GHz (100 GHz for the current protocol), and the increment in number of channels to 16 (4 or 8 channels for the current protocol).

While, in wavelength-division multiplexing (WDM) systems with higher speed or smaller channel spacing, for example, 25 Gb/s per channel or 50 GHz channel spacing, XPM is conceived as one of the main damages [10, 11]. Comparing with other nonlinear effect, for example the four-wave mixing (FWM) which can be easily suppressed by dispersion [12-14], there are few effective solutions to deal with the nonlinear phase modulation. In intensity modulation-direct detection (IM-DD) WDM systems, the XPM effect causes the spectrum broadens of the signal, resulting in the generation of different instantaneous light frequencies. Then, under the influence of group velocity dispersion (GVD), the generated different instantaneous light frequencies travel at different speeds in the optical fiber, leading to the irregular broaden of the signal waveform, i.e., the XPM-induced phase modulation is converted into intensity modulation, which may affect the transmission quality of the systems [15, 16]. In order to investigate the XPM effect, a large number of efforts can be found in literature. A. V. T. Cartaxo proposed a generalized model of the XPM-induced intensity modulation and verified its reliability by simulation [17]. X. Zhu et al. proposed an algorithm to estimate the power penalty brought by the XPM effect [18]. L. Paradiso evaluated the XPM effect by observing the spectrum [19]. Y. Song et al. experimentally studied the influence of the XPM nonlinear effect on the bit error rate (BER) of the 5G fronthaul network based on WDM-PON architecture [20]. For the mitigation of the XPM effect, researchers proposed a large number of solutions. S. Owaki et al. proposed a novel XPM compensation scheme based on neural

network, which successfully compensates the XPM distortion [21]. Q. Zheng et al. investigated a simple method at the receiver side for mitigating the XPM effect in WDM systems [22]. W. Lian et al. studied a nonlinear phase noise tracking algorithm to suppress the XPM effect in WDM systems [10]. While, few studies have been carried out so far for investigating the XPM effect on the upgraded NG-PON2 systems.

In this paper, the XPM effect on the upgraded NG-PON2 systems is studied. Three upgradation methods are proposed including the bit rate increment (10 Gb/s to 25 Gb/s per channel), channel spacing decrement (100 GHz to 50 GHz), and number of channels increment (8 to 16). For the first case of bit rate increment, the XPM-induced sensitivity penalty is 2.3 dB owing to the more-severe XPM effect induced by the bit rate increment. For the second case of channel spacing decrement, with the decrease of the channel spacing, a 0.4-dB sensitivity penalty is induced to the system. For the last case of number of channels increment, the XPM induces a negligible sensitivity penalty.

2. Theoretical analysis of the XPM effect

When two or more different wavelengths are propagating together in the same optical fiber, different frequencies would induce interferences due to the nonlinear effects of the optical fiber. For the XPM effect, it can be described as the intensity fluctuation of other channels modulates the phase of current channel by affecting the effective refractive index of the optical fiber. Here, the influence of the XPM effect on a two-channel system is analyzed as an example. For simplicity, it is assumed that the two wavelengths have the same polarization state and the polarization state remains unchanged during the transmission. Meanwhile, the GVD only causes the walk-off effect on the two wavelengths. Then, the coupled nonlinear Schrodinger equation of the two wavelengths can be described as follows [23]

$$\frac{\partial \mathrm{A}_1}{\partial \mathrm{z}}+\frac{1}{\mathrm{v}_{\mathrm{g1}}}\frac{\partial \mathrm{A}_1}{\partial \mathrm{t}}+\frac{\mathrm{i}\beta_{21}}{2}\frac{\partial^2 \mathrm{A}_1}{\partial \mathrm{t}^2}+\frac{\alpha_1}{2}\mathrm{A}_1=\mathrm{i}\gamma_1(|\mathrm{A}_1|^2+2|\mathrm{A}_2|^2)\mathrm{A}_1 \quad (1)$$

$$\frac{\partial \mathrm{A}_2}{\partial \mathrm{z}}+\frac{1}{\mathrm{v}_{\mathrm{g2}}}\frac{\partial \mathrm{A}_2}{\partial \mathrm{t}}+\frac{\mathrm{i}\beta_{22}}{2}\frac{\partial^2 \mathrm{A}_2}{\partial \mathrm{t}^2}+\frac{\alpha_2}{2}\mathrm{A}_2=\mathrm{i}\gamma_2(|\mathrm{A}_2|^2+2|\mathrm{A}_1|^2)\mathrm{A}_2 \quad (2)$$

where $\mathrm{A_j}$ is the slowly-varying amplitude, $|\mathrm{A_j}|^2$ denotes the power of the incident wavelength, $\mathrm{v_{gj}}$ refers the group velocity, $\beta_{2\mathrm{j}}$ describes the GVD, α_j represents the fiber attenuation coefficient, γ_j is the nonlinear coupling coefficient, and j=1, 2. In Eqs. (1) and (2), the first terms to the right of the equal sign denote the self-phase modulation (SPM) effect and the second terms represent the XPM effect.

The general solution of Eq. (1) can be expressed as

$$A_1(z,t)=A_1\left(0,t-z/v_{g1}\right)\exp\left(-\frac{\alpha z}{2}\right)\exp\left(i\emptyset_1(z,t)\right) \quad (3)$$

with

$$\emptyset_1(z,t)=\gamma_1\left[\frac{1-e^{-\alpha z}}{\alpha}\left|A_1(0,t-\frac{z}{v_{g1}})\right|^2+2\int_0^z\left|A_2(0,t-\frac{z}{v_{g1}}+d_{12}z')\right|^2e^{-\alpha z'}dz'\right] \quad (4)$$

where $\emptyset_1(z,t)$ is the SPM and XPM induced phase shift on Channel 1, $d_{12}\approx D\Delta\lambda_{12}$ denotes the walk-off parameter, D refers the GVD coefficient, and $\Delta\lambda_{12}$ means the channel spacing between Channel 1 and Channel 2.

Then, it is assumed that Channel 1 is an unmodulated signal and Channel 2 is modulated by sinusoidal signal, where the angular frequency is Ω_m. The optical power of Channel 1 and Channel 2 can be described as follows

$$P_1(0,t)=|A_1(0,t)|^2=P_{10} \quad (5)$$

$$P_2(0,t)=|A_2(0,t)|^2=P_{20}+P_{2m}\cos(\Omega_m t) \quad (6)$$

Substituting Eq. (5) and (6) into Eq. (4), the phase shift of Channel 1 ($\emptyset_1(L,t)$) can be expressed as

$$\emptyset_1(L,t)=\gamma_1(P_{10}+2P_{20})L_{eff}+\Delta\emptyset\cos(\Omega_m\left(t-\frac{L}{v_{g1}}\right)+\varphi) \quad (7)$$

where L_{eff} is the effective length of optical fiber and $\Delta\emptyset$ is the XPM index, which can be written as

$$\Delta\emptyset=2\gamma_1P_{2m}\sqrt{\eta_{XPM}}L_{eff} \quad (8)$$

with

$$\eta_{XPM}=\frac{\alpha^2}{{\Omega_m}^2d_{12}^2+\alpha^2}\left[1+\frac{4sin^2(\Omega_m d_{12}L/2)e^{-\alpha L}}{(1-e^{-\alpha L})^2}\right] \quad (9)$$

and

$$\varphi=cos^{-1}\frac{1-e^{-\alpha L}\cos(\Omega_m d_{12}L)}{\sqrt{(1-e^{-\alpha L})^2+4sin^2\left(\frac{\Omega_m d_{12}L}{2}\right)e^{-\alpha L}}}-cos^{-1}\frac{\alpha}{\sqrt{{\Omega_m}^2d_{12}^2+\alpha^2}} \quad (10)$$

where φ represents the phase delay factor associated with Ω_m. Thus, $\Delta\emptyset$ can be roughly expressed as

$$\Delta\emptyset\approx 2\gamma_1P_{2m}\alpha L_{eff}/\Omega_m D\Delta\lambda_{12} \quad (11)$$

Through the theoretical analysis, it is concluded that the XPM effect is closely related to the optical fiber parameters, the transmission distance, the modulation rate, the channel spacing, and the intensity of other wavelengths.

3. Simulation setup

In order to investigate the XPM effect on the upgraded NG-PON2 systems, we setup simulation systems using VPI Transmission Maker [20]. Moreover, the three upgradation options are considered in the simulations, as shown in Fig. 1. Due to that the system settings of the three upgradation options are similar, we describe the simulation setup of the bit rate increment case as an example. The used simulation parameters are represented in Table 1. At the transmitter side, 8 channels operating at 1596.3 nm~1601.9 nm (Channel 1 to Channel 8) are adopted as the optical carriers, whose channel spacing is 100 GHz and linewidth is 100 MHz. The 8 channels are given as following: 1596.3 nm, 1597.1 nm, 1597.9 nm, 1598.7 nm, 1599.5 nm, 1600.3 nm, 1601.1 nm, 1601.9 nm, respectively. Then, the optical carriers are modulated by 25 Gb/s non-return to zero (NRZ) signals through Mach-Zehnder Modulators (MZMs).

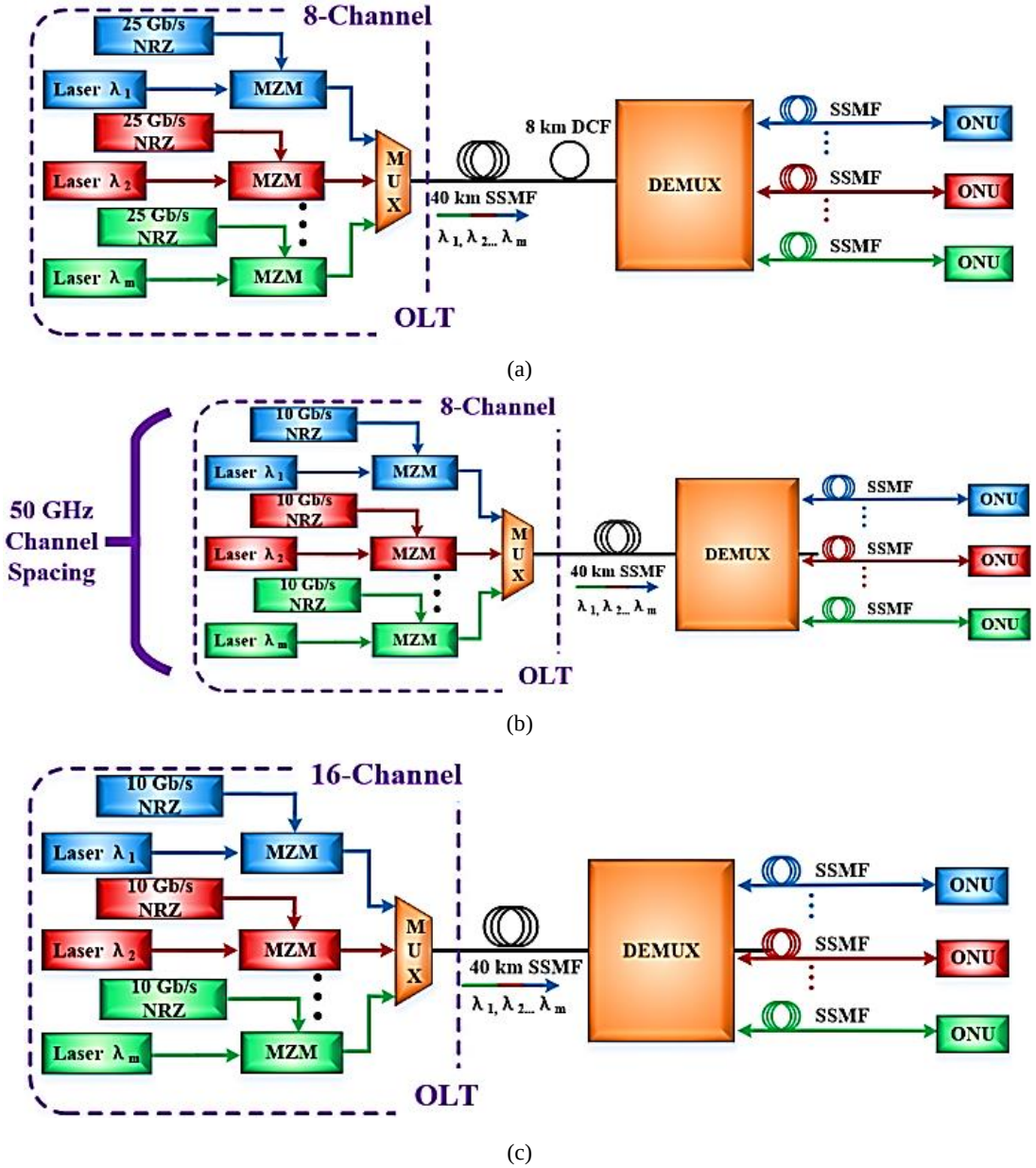

Fig. 1. Simulation schematic diagrams of the upgraded NG-PON2 systems when the (a) bit rate is increased to 25 Gb/s per channel, (b) channel spacing is decreased to 50 GHz, (c) number of channels is increased to 16 (color online)

The extinction ratio (ER) is 10 dB, the chirp coefficient is 0 and the output power is amplified to 8 dBm. When the signals are transmitting under the same polarization state, the XPM effect is conceived as the strongest. Therefore, all modulated channels are set in the same polarization state by polarization controllers (PCs). Subsequently, the 8 channels are coupled together by a multiplexer (MUX), whose insertion loss is 1.5 dB and pass band isolation is 30 dB. In order to accumulate the maximum of the XPM effect, the length of the standard single mode fiber (SSMF) is selected as 40 km. The dispersion coefficient, fiber attenuation, and dispersion slope are 20 ps/nm·km, 0.2 dB/km, and 0.08 ps/nm^2·km, respectively. Considering the random change of the polarization states for different wavelengths caused by the SSMF, the polarization states of all the channels shall be different during the real simulations. Note that, in the first case of the bit rate increment, for achieving 40 km transmission distance, dispersion compensation fiber (DCF) is employed to compensate the dispersion. The dispersion coefficient of the DCF is -100 ps/nm·km and the link length is 8 km. While, in the other two cases, DCF is not used. Afterwards, the coupled signals are injected into a de-multiplexer (DEMUX) for filtering. The insertion loss and pass band isolation of the DEMUX are 1.5 dB and 30 dB, respectively. Here, Channel 4 (Channel 5) is filtered by a DEMUX as the target channel since it is in the middle of the 8 signals, indicating that it suffers greater XPM effect than other signals. At the receiver side, the signal of Channel 4 is firstly detected by an avalanche photodiode (APD) receiver and finally captured by the BER Analyzer module for further analysis. The dark current and responsivity of the APD are 2×10^{-8} A and 0.9 A/W, respectively. In order to obtain the XPM-induced sensitivity penalty, we also transmit the single wavelength of Channel 4 under the same condition as a comparison.

Table 1. Simulation Parameters for upgraded NG-PON2

Parameters	Value
Number of Channels	8, 16
Channel Spacing	100 GHz, 50 GHz
Modulation Rate	25 Gb/s, 10 Gb/s
Fiber Attenuation	0.2 dB/km
Dispersion Slope	0.08 ps/nm^2·km
Chirp Coefficient	0
Out Power	8 dBm per channel
Fiber Length	40 km
Dispersion Coefficient	20 ps/nm·km
APD Dark Current	2×10^{-8} A
APD Responsivity	0.9 A/W

4. Simulation results and analysis

Firstly, we analyze the XPM-induced sensitivity penalty when the bit rate is increased to 25 Gb/s, as given in Fig. 2. It can be seen that, when the wavelengths are simultaneously transmitted 40 km SSMF, the obtained sensitivity is -21 dBm at the case of 1×10^{-3} BER (considering the 7% hard decision-forward error correction and the tolerance away from the worst case) [24]. While, when the single wavelength of Channel 4 is transmitted 40 km SSMF, the obtained sensitivity is -23.3 dBm. Therefore, the XPM-induced sensitivity penalty is measured as 2.3 dB. It is due to that, with the increase of the bit rate, the XPM effect becomes more severe, resulting in an extra sensitivity penalty, which is consistent with the theoretical analysis.

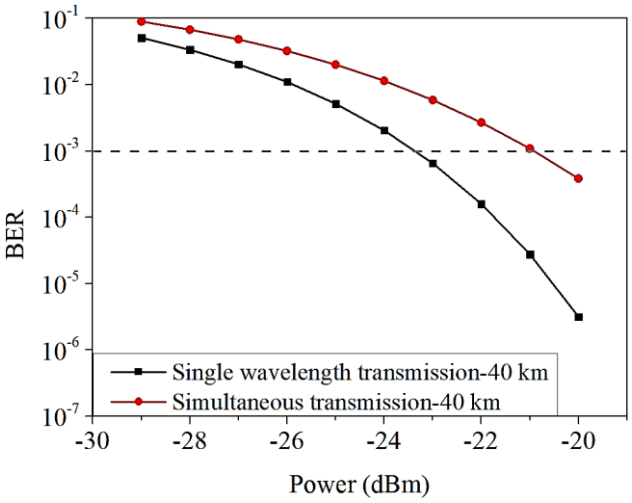

Fig. 2. The measured BER curves of Channel 4 after the single wavelength and simultaneous transmission when the bit rate is increased to 25 Gb/s per channel (color online)

Then, Fig. 3 represents the measured BER curves of Channel 4 when the channel spacing is decreased to 50 GHz. According to the theoretical analysis, the XPM effect increases with the decrease of the channel spacing. When the wavelengths simultaneously passing through 40 km SSMF, the obtained sensitivity is -26.2 dBm (1×10^{-3} BER). By contrast, when the single wavelength of Channel 4 is passing through 40 km SSMF, the obtained sensitivity is -26.6 dBm, resulting in a 0.4-dB sensitivity penalty.

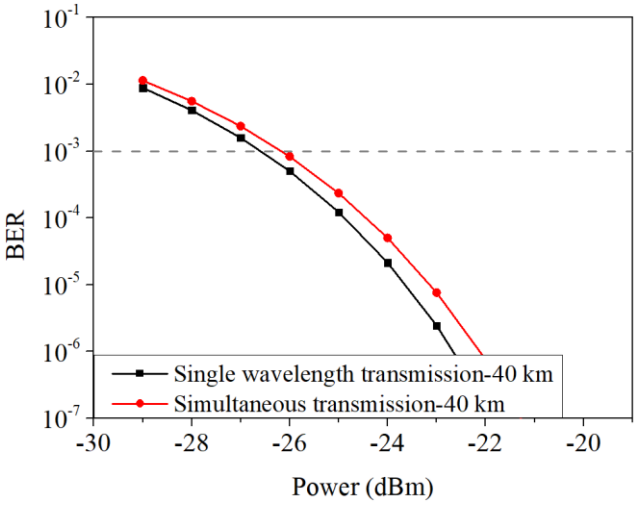

Fig. 3. The measured BER curves of Channel 4 after the single wavelength and simultaneous transmission when the channel spacing is decreased to 50 GHz (color online)

Finally, Fig. 4 depicts the measured BER curves of the target channel (Channel 8 in this case) when the number of channels is increased to 16. It can be seen that, although the number of channels increases, the larger-spaced channels have little effect on Channel 8, resulting in an ignorable sensitivity penalty. Therefore, when the wavelengths are simultaneously passing through 40 km SSMF, the obtained BER is similar to that of the single wavelength transmission of Channel 8.

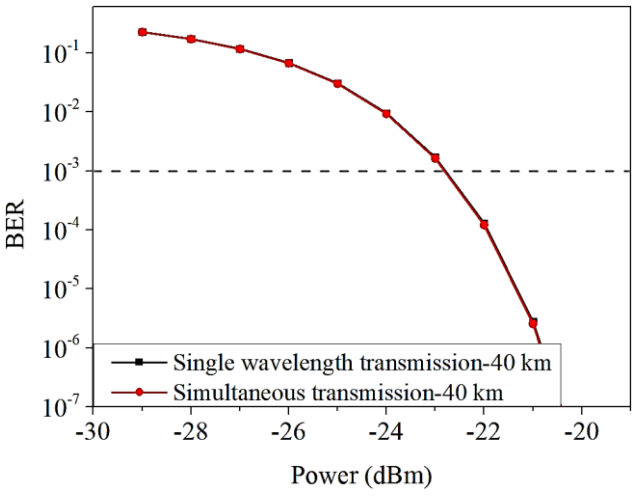

Fig. 4. The measured BER curves of Channel 8 after the single wavelength and simultaneous transmission when the number of channels increases to 16 (color online)

5. Conclusion

In this paper, the influence of the XPM effect on the upgraded NG-PON2 systems is investigated through simulations. Three upgradation options are proposed, which include the bit rate increment to 25 Gb/s per channel, the channel spacing decrement to 50 GHz, and the increment in number of channels to 16. For the bit rate increment case, the XPM-induced sensitivity penalty is 2.3 dB. For the channel spacing decrement case, a 0.4-dB sensitivity penalty is induced by the XPM effect. For the number of channels increment case, the XPM effect causes an ignorable sensitivity penalty.

References

[1] V. Houtsma, V. D. Veen, J. Lightw. Technol. **35**(4), 1059 (2016).
[2] A. Saleem, H. Cui, Y. He, A. Boag, IEEE Antennas and Propagation Magazine, **64**(3), 126 (2022).
[3] G. Liu, L. Zhang, T. Zuo, Q. Zhang, J. Zhou, E. Zhou, Opt. Fiber Commun. Conf. Exhib., Th3D.5 (2017).
[4] A. Saleem, Y. Xu, R. A. Khan, I. Rasheed, Z. A. Jaffri, M. A Layek, Wireless Communications and Mobile Computing, **2022**, 9090494 (2022).
[5] V. Houtsma, V. D. Veen, J. Lightw. Technol. **21**(3), 587 (2013).
[6] J. A. Altabas, O. Gallardo, G. S. Valdecasa, M. Squartecchia, D. Izquierdo, S. Sarmiento, M. Barrio, J. A. Lazaro, I. Garces, J. B. Jensen, 22nd International Conference on Transparent Optical Networks (ICTON), Mo.D1.4 (2020).
[7] V. Houtsma, A. Mahadevan, N. Kaneda, D. van Veen, J. Opt. Commun. Netw. **13**(1), A44 (2021).
[8] D. Nesset, J. Opt. Commun. Netw. **9**(1), A71 (2017).
[9] V. Houtsma, D. van Veen, S. Porto, N. Basavanhally, C. Bolle, Opt. Fiber Commun. Conf. Exhib. M1B.3 (2018).
[10] W. Lian, Q. Zheng, W. Li, Y. Wang, Opt. Commun. **474**, 126184 (2020).
[11] Anamik, V. Priye, Opt. Fiber Technol. **19**(2), 75 (2013).
[12] P. P. Mitra, J. B. Stark, Nature **441**, 1027 (2001).
[13] S. Ten, K. M. Ennser, J. M. Grochocinski, S. P. Burtsev, V. L. daSilva, Proc. Optical Fiber Conf, 43-45 (1999).
[14] X. Wu, Z. Li, Y. Song, Y. Guo, Y. Yin, M. Wang, Opt. Commun. **403**, 335 (2017).
[15] Y. Xu, P. Yu, N. Ye, Y. Song, Opt. Eng. **60**(4), 046105 (2021).
[16] M. Wang, J. Zhang, J. Mod. Optic. **61**(13), 1039 (2014).
[17] A. V. T. Cartaxo, IEEE Photonic Tech. L. **10**(9), 1268 (1998).
[18] X. Zhu, Q. Zeng, Chin. Opt. Lett. **1**(5), 263 (2003).
[19] L. Paradiso, P. Boffi, L. Marazzi, G. Pozzi, M. Artiglia, M. Martinelli, IEEE Photonic Tech. L. **17**(1),

160 (2005).
[20] Y. Song, P. Yu, Y. Xu, Z. Li, Opt. Fiber Technol. **65**, 102628 (2021).
[21] S. Owaki, M. Nakamura, IEICE Commun. Express **7**(1), 31 (2018).
[22] Q. Zheng, W. Li, R. Yan, Q. Feng, Y. Xie, Y. Wang, IEEE Photonics J. **11**(6), 7205411 (2019).
[23] G. P. Agrawal, Nonlinear Fiber Optics, 5th Edition, Rochester, New York, 2013.
[24] T. Xu, Z. Li, J. Peng, A. Tan, Y. Song, Y. Li, J. Chen, M. Wang, IEEE Photonics J. **10**(4), 7905508 (2018).

*Corresponding author: Beryly@shu.edu.cn